The Thermal Pulses of Very-Low-Mass Stars

Alfred Gautschy, CBmA Liestal and ETH-Bibliothek Zürich

March 28, 2013

Very-low-mass stars can develop secularly unstable hydrogen-burning shells late in their life. Since the thermal pulses that go along are driven at the bottoms of very shallow envelopes, the stars' luminosities and effective temperatures react strongly during a pulse cycle. Towards the end of the Galaxy's stelliferous era, the hydrogen-shell flashing very-low-mass single stars should inflict an intricate light-show performed by the large population of previously inconspicuous dim stars. Unfortunately, this natural spectacle will discharge too late for mankind to indulge in. Not all is hopeless, though: In the case of close binary-star evolution, hydrogen-shell flashes of mass-stripped, very-low mass binary components can develop in a fraction of a Hubble time. Therefore, the Galaxy should be able put forth a few candidates that are going to evolve through a H-shell flash in a humanity-compatible time frame.

The Evolution of Single Very-Low-Mass Stars

Red dwarfs in the mass range of about $0.08 - 0.45\,M_\odot$, referred to as very-low-mass (VLM) stars hereafter, are massive enough to start nuclear burning of hydrogen but *not* massive enough to enter the stage of helium burning; these stars do not rank highly as daring astrophysical objects. Indeed, most or all of their life is quiet and dim, or put otherwise: unspectacular. For most of the nuclear lifetime of the VLM stars, which exceeds the current age of the Universe by a large margin, they stay put close to the main sequence on the low luminosity and low effective-temperature corner of the HR diagram. In particular the low-mass fraction of the red dwarfs, which remains essentially fully convective during most of the main-sequence phase, feeds the nuclear-burning core with fresh fuel from throughout the whole stellar volume for a long time, ranging from about 100 Gyrs for $\approx 0.4M_\odot$ to more than 1000 Gyrs for $\approx 0.15M_\odot$ stars.

Only those VLM stars that develop radiative cores at some stage during central hydrogen burning ascend the 1st giant branch noticeably, i.e. VLM stars with $M_* \gtrsim 0.15M_\odot$ inflate at least somewhat. Since stars with $M_* \lesssim 0.45M_\odot$ do not ignite core helium burning, they leave the giant branch once the envelope mass (i.e. the mass above the slowly outward-eating hydrogen burning shell) drops below a critical value. Both, the reduction of envelope mass and the ever increasing stellar radius of the stars ascending the red-giant branch both contribute to the reduction of the total pressure at the hydrogen-burning shell so that eventually $T_{\rm eff}$ must increase in order to be able to transport to the surface the energy generated at the H-shell. The luminosity at which the VLM stars divert from the fiducial giant branch correlates with the total stellar mass: The

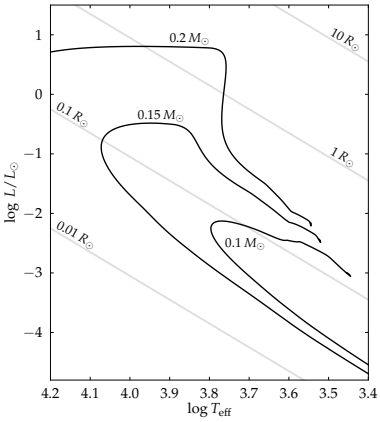

Figure 1: Examples of VLM evolutionary tracks – 0.1, 0.15, and $0.2M_\odot$ with $Z = 0.02$ – on the HR plane.

Numerical data cited in the text without explicit reference refer either to results from own computations with the MESA stellar evolution code (cf. Appendix) or are considered to be part of the current astronomical canon.

higher the total mass, the brighter the giant upon departure from the giant branch; at the same time, the remaining relative envelope mass diminishes.

After leaving the giant branch, the VLM stars cross the HR diagram at about constant luminosity and evolve to effective temperatures exceeding 10^4 K, see e.g. Fig. 1. Again, the maximum temperature correlates with the stellar mass in such a way that higher mass stars achieve higher maximum $T_{\rm eff}$. The crossing at constant luminosity ($\Delta t = \mathcal{O}(10^8 - 10^9)$ years for $0.2\,M_\odot$ and $\mathcal{O}(10^7)$ years for $0.35\,M_\odot$, subject to composition and the particular microphysics invoked) and the early cooling along the characteristic cooling helium white-dwarf branch are quick compared with the earlier stages of evolution. The horizontal evolution at constant luminosity terminates once the previously generated luminosity, in accordance with the core-mass – luminosity relation, can be maintained in the ever less massive hydrogen-burning shell which already gets cooler as the star heats up at the surface.

With the luminosity support of the weaker-getting hydrogen-burning shell the VLM stars approach the helium-white-dwarf cooling region. Not all VLM stars evolve monotonously through the early degenerate cooling phase; for some, the hydrogen shells undergo one or several thermal flashes. Since the secularly unstable hydrogen-burning shells lie at the bottoms of only very shallow envelopes the respective stars react sensitively and embark on complicated trajectories on the HR diagram.

Hydrogen Shell Flashes in VLM Stars

The central part of this exposition focuses on the *thermally pulsing* VLM stars; we are going to look into the physical circumstances of the H-shell flashes and their rôle in stellar astronomy of single VLM stars and as components in close binary systems as observable currently.

Figures 2 to 4 all show evolutionary tracks of selected model sequences, first with changing heavy element abundance, and then illustrating the effect of elemental diffusion. Each figure contains evolutionary tracks of stars just above and below the secularly unstable mass range in gray; two selected thermally pulsing representants in between illustrate topology and extent of the tracks that result as a reaction on the H-shell flashes.

Non-diffusive star models

To start, we focus first on the results of *simple* evolutionary computations, meaning in the present context neglecting elemental diffusion. Independent of the stars' metallicity, there exists always a range of stellar masses within which the physical circumstances were favorable for the stars to develop secularly unstable H-shell burning early on the white-dwarf cooling track.[1] As a consequence,

[1] Historically, Kippenhahn et al. (1968) were the first to encounter a hydrogen-shell flash in a low-mass star. The authors were interested in following the long-time evolution of an interacting binary system, simulated with a single-star evolution code. To learn about later work on this topic see e.g. Driebe et al. (1998), Sarna et al. (2000), Benvenuto & De Vito (2005) and references therein.

the secularly unstable models underwent one or a few hydrogen flashes, which forced them to loop extensively on the HR plane. The *magnitude* and *topology* of the excursions away from the evolutionary tracks as traced out by stars burning hydrogen quietly depended on stellar mass as well as on chemical composition. The particularities of the microphysics treatment, as well as the chemical composition influenced the mass range of stars that underwent hydrogen shell flashes.

In the case of solar-like $X = 0.7, Z = 0.02$ models, secularly unstable H-shells were encountered in the range from 0.19 to $0.32 M_\odot$. The thermal flashes are most vigorous close to the lower mass boundary. Between 0.19 and $0.2 M_\odot$ the model sequences passed through four hydrogen-shell flash cycles. From 0.26 to $0.32 M_\odot$, only one single hydrogen flash took place. Selected evolutionary tracks illustrate the situation in Fig. 2.

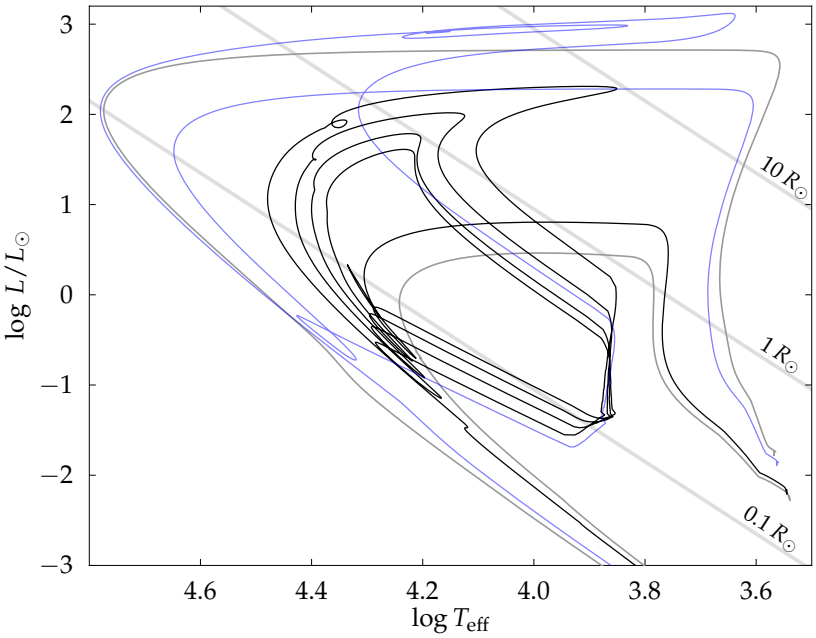

Figure 2: Evolutionary tracks on the HR plane of $Z = 0.02$ VLM models. The two gray tracks are traced by a $0.185\,M_\odot$ model on the low-mass and a $0.35\,M_\odot$ model on the higher-mass side; these two stellar masses bracket the domain of the thermal pulsing instability. For illustration, the fine black line, including four thermal pulses, shows the track of a $0.2\,M_\odot$ model. The blue line is traced out by a $0.3\,M_\odot$ model, which lives through only one thermal pulse of the H-burning shell anymore.

Of the four tracks included in Fig. 2, the two gray ones delineate roughly the upper ($0.35\,M_\odot$) and lower ($0.185\,M_\odot$) mass boundary in between of which the unstable hydrogen shells were encountered. The black locus is indicative of a multi-flash cycling VLM star – here a $0.2\,M_\odot$ model sequence evolving through four cycles. The blue-colored evolutionary locus shows the example of a star close to the upper mass boundary for unstable hydrogen burning; these stars, although only living through a single pulse can pass through a very puffed-up born-again red-giant phase before they settle again on the quiet white dwarf cooling track. For better illustration of the amount of radius growth during hydrogen flashes, lines of constant radii are added to the plot. Notice that during the flash-induced excursions on the HR plane, the radii of these VLM stars can grow temporarily ten- to hundredfold.

Figure 3 is closely related to Fig. 2 but shows evolutionary tracks on the HR plane of selected star models with $X = 0.757, Z = 0.001$. The tracks are shown from their starting as thermally contracting, homogeneous gas spheres at the Hayashi line which then approach the main sequence before they set out on the same evolutionary voyage as the models in Fig. 2.

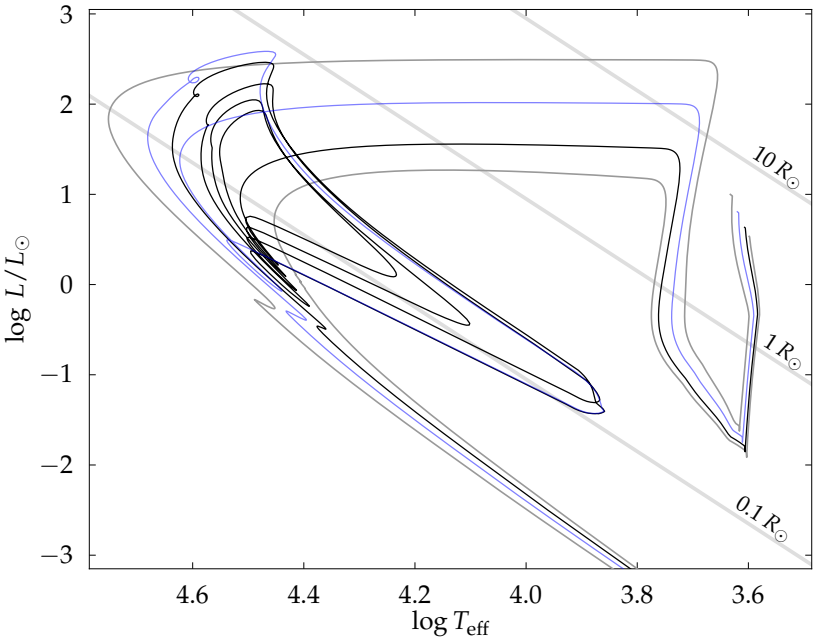

Figure 3: Evolutionary tracks of $Z = 0.001$ VLM models on the HR plane. The two gray tracks are traced out by a $0.24\,M_\odot$ model on the low-mass and a $0.355\,M_\odot$ model on the higher-mass side. These two stellar masses bracket the domain of the thermal pulsing instability. For illustration, the fine black line, including four thermal pulses, shows the track of a $0.26\,M_\odot$ model. The blue locus is traced out by a $0.3\,M_\odot$ model, which lives through only one thermal pulse of the H-burning shell anymore.

The metal-poor VLM models showed also a range of stellar masses with secularly unstable hydrogen shells. Starting at $0.25M_\odot$, up to $0.26M_\odot$, with four thermal flash cycles, the temporarily unstable hydrogen-burning shells persisted up to $0.35M_\odot$. Figure 3 shows in gray quietly H-burning model sequences with 0.24 and $0.355M_\odot$, jammed in between is a model evolving through four hydrogen-shell flashes (in black) and a model sequence (in blue) close to the upper mass boundary encountering a single thermal flash.

Phenomenologically, the major difference between the $Z = 0.001$ and the $Z = 0.02$ models is the reduced radius change encountered during a hydrogen shell flash by the metal-poor star models. Reminiscent of other situations in stellar astronomy, metal poor star tend to prefer the bluer parts of the HR diagram as compared to the metal richer populations. Most pronounced we see this manifested in the lacking red noses – compare Fig. 3 with Fig. 2 – of the evolutionary tracks at high luminosity during the hydrogen flashes. The metal poor VLM stars do not produce born-again red giants but only bright blueish giants.

Models with elemental diffusion

The nuclear-evolution timescale of single VLM stars is very long, exceeding the current age of the Universe. Hence, these stars are

candidates for diffusion to play a rôle for structure and evolution as soon as radiative regions develop in their interiors. For the illustrative purposes of this exposition, we computed a set of $Z = 0.02$ models to get a rough impression of the effect of elemental diffusion on existence and prevalence of the H-shell flashes and surface character of diffusive model stars.

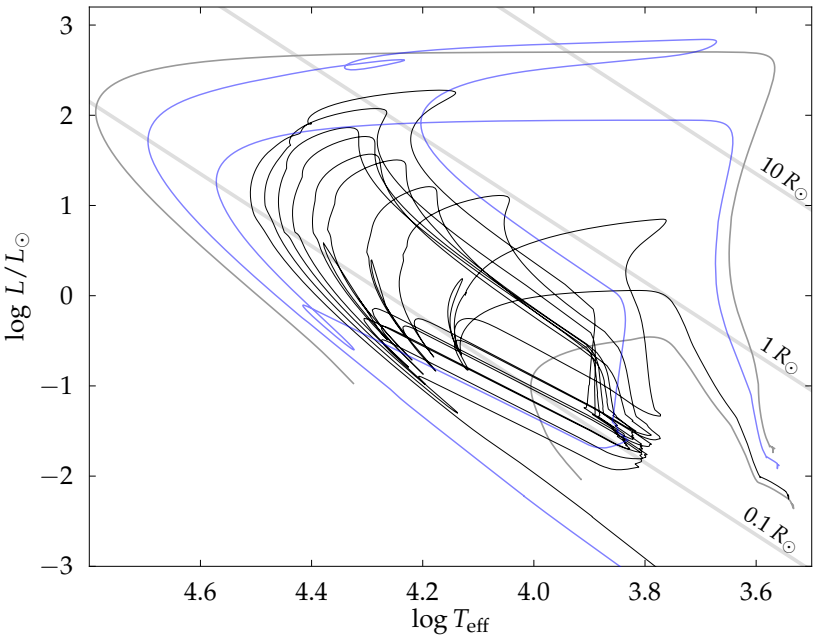

Figure 4: Evolutionary tracks of $Z = 0.02$ *diffusive* VLM models on the HR plane. The two gray tracks are traced by a $0.17\,M_\odot$ model on the low-mass and a $0.37\,M_\odot$ model on the high-mass side of the secular instability domain. For illustration, the thin black line, including nine thermal pulses, shows the track of a $0.19\,M_\odot$ model. The blue line is traced out by a $0.29\,M_\odot$ model, which lives through only one thermal pulse of the H-burning shell anymore.

Figure 4 shows, in the same spirit as Figs. 2 and 3, selected evolutionary tracks of star models with $Z = 0.02$, which were computed including elemental diffusion. The gray lines belonging to the $0.17M_\odot$ and the $0.37M_\odot$ tracks trace out the lower and upper boundary in between of which stars undergo hydrogen-shell flashes. In contrast to the diffusion-free models, thermal flashes are more numerous when elemental diffusion affects the stars' abundance stratification. The maximum number of 9 thermal pulses was encountered in the case of the $0.19M_\odot$ model star, its track is shown as the black line in Fig. 4. The example of a star with $0.29M_\odot$, close to the upper mass-boundary of H-shell instability, undergoing only a single hydrogen shell flash with an extensive excursion into the red-giant region is also included in Fig. 4; its track is shown with the blue line. Comparing the blue tracks of Fig. 2 and Fig. 4 makes clear that evolutionary tracks of the single H-shell flash stars do not diverge strongly; hence, the effect of elemental diffusion on the phenomenology of the tracks is minimal.

The bolometric lightcurve of the thermally pulsing $0.19\,M_\odot$ star of Fig. 4 is displayed in Fig. 5. The abscissa measures the time in mega-years relative to the arbitrary, but convenient epoch at $t = 1.074 \times 10^{12}$ years, measuring roughly the age of the model star on the top of the 1$^{\rm st}$ giant branch. The lightcurve shown in Fig. 4 makes it clear that the thermal pulses induced by the hydrogen-

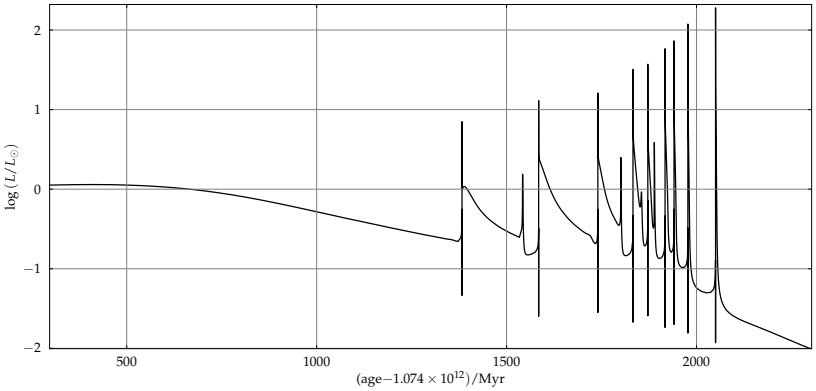

Figure 5: Temporal evolution of the luminosity of a $0.19\,M_\odot$, $Z = 0.02$ model star around the evolutionary stage of secularly unstable hydrogen shell burning. For convenience, the plotted age of the star is offset by 1.074×10^{12}; on this scale, giant-branch evolution of the star terminates around 500.

burning shell are quite irregular, much more so than those of He-shell flashes. The interpulse-period can range from 202 Myrs (between pulse 1 and 2) to 24 Myrs (from pulse 6 to 7). The amplitude of the pulses, though, grow continuously. During the first pulse, the luminosity rises by about $100\,L_\odot$; then, during the last pulse, the luminosity amplitude grows to about $10\,000\,L_\odot$. The lightcurves of the thermal-pulse phase reflects also the complicated loci traced out by the model star on the HR plane (see Fig. 4). We observe considerable substructure in a thermal pulse; an aspect which got some attention in Driebe et al. (1999). [2] The substructures within a particular pulse cycle do, however, not necessarily repeat in subsequent cycles. It can even be tricky, based on the luminosity variation alone, to determine when a cycle has finished. Analyzing the track on the HR plane, though, resolves this problem.

The He-shell flashes that occur in stars along the asymptotic giant branch are computed to be much more regular (e.g. Iben 2013, Chapter 18.3); they even follow a reliable correlation of core mass and inter-pulse period (Paczyński 1975).

[2] The stellar modeling used in Driebe et al. (1999) did not include elemental diffusion; the range of stellar masses found to encounter H-shell flashes, $0.21 - 0.3\,M_\odot$, compares favorably with our diffusion-less model sequences.

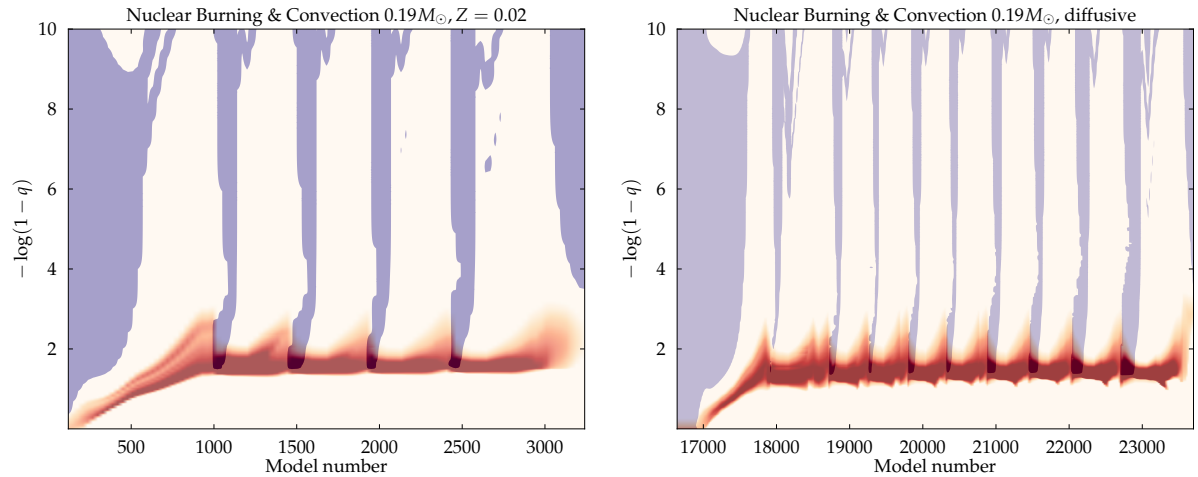

Figure 6: Kippenhahn diagrams tracing out the convection zones (blue) and the strength of nuclear burning (red) of $0.19\,M_\odot$ model stars. The left panel shows the case of a *non-diffusive* model, the right panel contains the result from modeling the star inclusive *elemental diffusion*.

THE KIPPENHAHN DIAGRAMS of Fig. 6, plotting $-\log(1-q)$ with $q = m/M_*$, i.e. measuring the remaining relative mass lying above a given mass coordinate, versus model number to appropriately but non-monotonously stretch the time axis, show the behavior of a non-diffusive $0.19\,M_\odot$ model in the left and a diffusive model of the same mass in the right panel. The chosen model numbers in the panels

essentially zoom in to the evolutionary window between the end of core hydrogen burning and the termination of hydrogen shell flashes when also nuclear energy generation dies out. Model numbers of the non-diffusive model stars shown in the left panels of Figs. 6 and 7 can be related to physical ages using the table on the margin. For the diffusive case, correlating the thermal flashes in Fig. 5 with the associated convection fingers in Fig. 6 does the job.

Model	age/10^{12} yrs
500	1.15053
1000	1.15082
1500	1.15084
2000	1.15086
2500	1.15089
3000	1.15131

The shades of red in Fig. 6 indicate nuclear burning with deeper red meaning higher specific nuclear energy generation rate; the particular magnitudes are of no interest here. Blue regions map out convection zones (according to Schwarzschild's criterion); in the remaining pale the background, energy is transported by radiation diffusion. The big blue patches on the left of both panels indicate the fully convective red dwarfs and the red-giant phase with its very deep convective envelopes on top of the hydrogen-burning shell. The thin convective branches, in the region $8 \lesssim -\log(1-q) \lesssim 10$, growing out of the dominating vertical convection trunks are the robust convection zones induced by partial hydrogen and helium ionization; the superficial convection zones persist even when essentially the whole envelope becomes radiative when the model stars heat up. Depending on the prevailing density structure in the stellar envelope, the zones merge or appear as separate thin convection zones. The patchy convective regions, appearing only during the late thermal-pulse phase, deeper in the stars' envelopes ($6 \lesssim -\log(1-q) \lesssim 8$) are attributable to the Fe-bump of the opacity. At sufficiently high envelope density, the local opacity peak can push up $\nabla_{\rm rad}$ to make the region superadiabatic and hence convectively unstable.

The hydrogen-shell flashes are not only discernible as temporarily extended and stronger nuclear-burning regions in Fig. 6 but also by the ensuing deep convection zones which reach into the nuclear burning region of the star models (except for the first pulse in the diffusive model). Such deeply penetrating convection means that nuclearly processed material (CNO-cycle processed in the current case) will be dredged up to the stellar surface.

For the same models and the same evolutionary window as shown in Fig. 6, the temporal evolution of the hydrogen abundance stratification of non-diffusive (left panel) and diffusive models (right panel) are illustrated in Fig. 7. The white bottom regions of the two panels measure the mass of the degenerate, nuclear inactive helium core.

Notice that the deepest blue coloring amounts to different maximum hydrogen abundances in the left and the right panel, respectively.

In accordance with the convection zones and the nuclear burning, in particular during the hydrogen-shell flashes, the left panel of Fig. 7 shows a discontinuous hydrogen depletion in the stars' envelope as the star model passes through its four thermal pulses. The process starts at the low, spatially homogeneous value of $X \approx 0.3$ at the end of core hydrogen burning; X is so low because the $0.19\,M_\odot$ model stayed fully convective for a significant fraction of its main-sequence lifetime so that about half of the star's *total* hydrogen con-

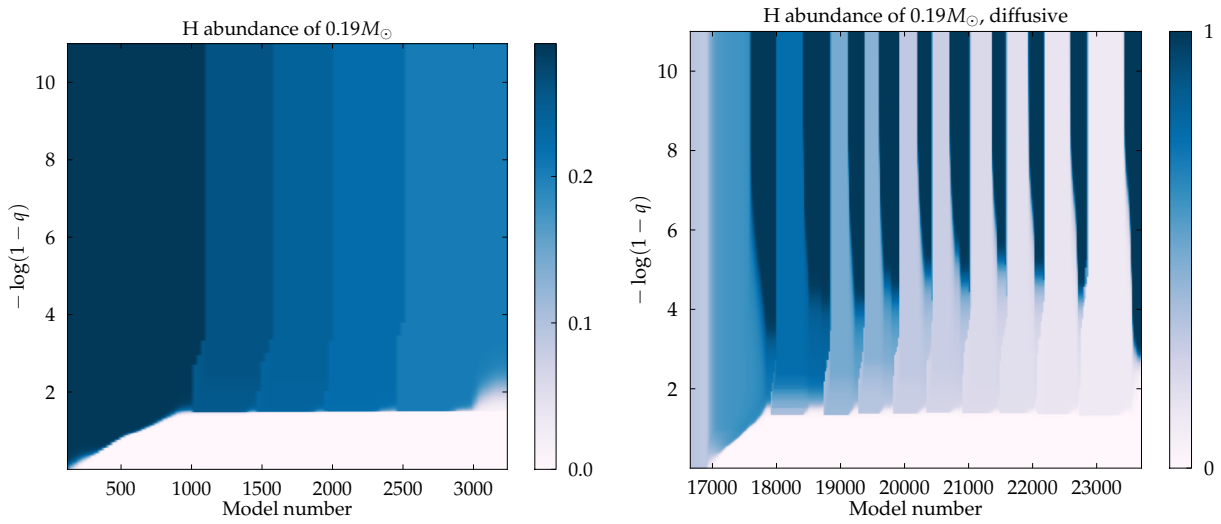

Figure 7: Kippenhahn diagrams showing the spatial evolution of the hydrogen abundance of 0.19 $M_\odot$ model stars.

tent was consumed during its main-sequence phase. The envelope hydrogen abundance remains constant up to the first thermal flash when a fraction is burned up and the remaining X abundance is homogenized via convection through the stellar envelope. With each further thermal flash the star's hydrogen abundance gets reduced and homogenized; this process produces the patchy sequence of ever lighter blue tones in the left panel of Fig. 7. The temporal evolution of the abundance stratification is more complex in diffusive models. The right panel of Fig. 7 illustrates that elemental diffusion is effective enough that between all H-flashes, when deep convection ceases, hydrogen diffuses to the top of the star. Hence, chemically the H-flashing star appears alternately as a H-depleted or even a helium star (during a flash) or a star with a thin essentially pure hydrogen envelope. The thickness of the superficial hydrogen layer in diffusive models, of the order $10^{-4} - 10^{-6}\,M_*$, is much thinner than in the case if elemental diffusion is neglected.

Evolution of the surface abundances of hydrogen (black), ^{12}C (blue), and ^{16}O (red) are displayed for non-diffusive star models in the left and for models including elemental diffusion in the right panel of Fig. 8.

Evidently, the spectral appearance of old VLM stars, in particular during the thermal-pulse episode, is different for diffusive and diffusion-free models. In the latter case the hydrogen abundance decreases monotonically in time; during each H-shell flash it drops quickly – leading to a step in Fig. 8. Hydrogen depletion starts already during core hydrogen burning due to the star's fully convective structure; once the star arrives on the white-dwarf cooling-track, it evolves into an increasingly more pronounced hydrogen-deficient white dwarf. Parallel to hydrogen, also the abundances of ^{12}C and ^{16}O diminish on the surface, with the ratio C/O sinking from about 0.36 to roughly 0.02 after the thermal pulses. Models with diffusion present a less monotonous picture. During the H-shell pulses, when the envelope is convective, the surface hydrogen

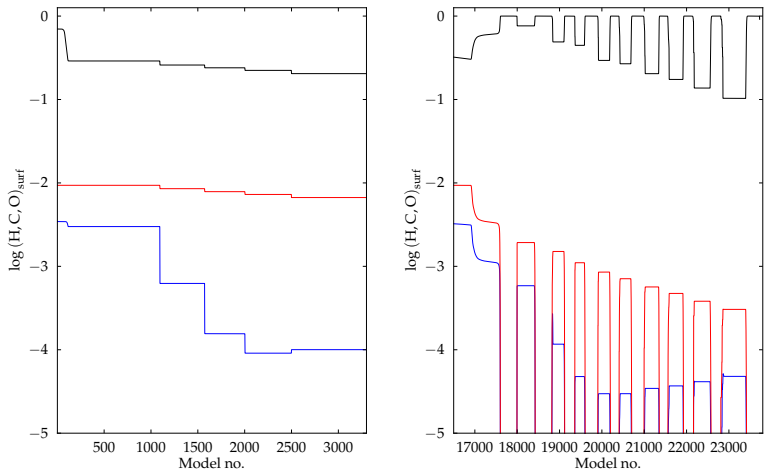

Figure 8: Comparison of the temporal evolution of the surface abundances of hydrogen (black), ^{12}C (blue), and ^{16}O (red) of the $Z = 0.02, 0.19\,M_\odot$ model series without diffusion (left panel) and including elemental diffusion (right panel).

abundance is lower than in the diffusion-free models. As soon as the envelope becomes radiative again – during most of the interpulse phase – elemental diffusion strongly modifies the superficial abundance structure. The envelopes get purified in the sense that the superficial layers consist then essentially of pure hydrogen. Each interpulse period is long enough for this purification to take effect. Hence, either the thermally pulsing VLM stars are observable as hydrogen-deficient, with their hydrogen-deficiency to grow with advancing age and with decreasing luminosity (if the star is not on an extended tour of the HR plane as a consequence of the H-shell flash), or the VLM stars of a large range of luminosities, lying along the white-dwarf cooling track, show a black-body spectrum with an overlaid chiefly pure hydrogen line-spectrum. The temporal evolution of the abundances of ^{12}C and ^{16}O show the mirror image of that of hydrogen. During the phases of convective envelopes the C and O abundances at the surface build up, during radiative phases of the envelope these heavier elements diffuse inward and essentially disappear from the surface. The general trend of reducing the C (at least up to the 5^{th} pulse) and the monotonous reduction of O across all thermal pulses is functionally comparable to the diffusion-free case. However, if elemental diffusion is accounted for, the magnitude of reduction across the thermal-pulse phase is much larger. Also the C/O ratio changes differently. The ratio starts at about 0.35 before the thermal pulses set in; around the 4^{th} pulse C/O reaches a minimum at 0.04 to rise back to about 0.16 when the star reaches its terminal cooling phase.

The Physics of Hydrogen Shell Flashes

Not long after the first encounter of H-shell flashes in VLM stars (Kippenhahn et al. 1968) the phenomenon was physically analyzed and explained Giannone & Weigert (1967)[3] expanding on the ansatz of Schwarzschild & Härm (1965).

Giannone & Weigert (1967) asked under what conditions a heat perturbation continues to grow if it is applied to a thin nuclear

[3] The violation of causality is only ostensible: Kippenhahn et al. (1967) was the precursor paper to Kippenhahn et al. (1968); the earlier paper computed the evolution of the initially $2.0\,M_\odot$ primary star of a close binary system to the point of onset of the secular instability of the hydrogen-burning shell when the primary was stripped down to $0.26\,M_\odot$. Weigert, working in the Kippenhahn group and having come across helium-shell flashes in intermediate mass stars earlier, was well prepared to apply his expertise to secular instabilities of *hydrogen-burning* shells.

burning shell. The reaction of the nuclear active shell and the form of the perturbations were highly abstracted, but the method allowed to formulate simple analytical conditions that are to be met for *secular instability* to develop. Derived from the linear stability analysis of the energy and the transport equation, the following two criteria are necessarily to be fulfilled: *The shell must be thin enough*:

$$D_1 \equiv 4\,[\alpha - \nabla_{\rm ad}\cdot\delta]\cdot\frac{\Delta r}{r} < 1\,, \tag{1}$$

but at the same time, *the shell must not be too thin*:

$$D_2 \equiv \frac{8}{\Delta\ln T\cdot\varepsilon_T\cdot(\Delta L/L)} < 1\,. \tag{2}$$

The pair $\{P,T\}$ is adopted as the thermodynamical basis; the characteristic exponents of the equation of state, α and δ, are related to the parametrization $\rho \sim P^{\alpha}T^{-\delta}$. The variation of physical quantities q across the nuclear burning shell are written as Δq. The rest of the symbols has canonical meaning, following closely the usage in (Kippenhahn & Weigert 1994).

The condition of the shell to be thin enough – Eq. (1) – ensures that the pressure reaction during expansion (after some heat perturbation be applied to the nuclear burning shell) remains sufficiently weak so that the temperature in the shell to continues to grow. Equation (2) on the other hand must ensure that the shell is not too thin in order for the heat perturbation to remain contained in the shell. This can be accomplished either by a sufficiently strong nuclear burning (manifested through the magnitude of ε_T and ΔL, the luminosity contrast across the shell) or then by sufficiently weak energy leakage, measured by the temperature contrast $\Delta\ln T$ through the thin nuclear-burning shell.

Both conditions, D_1 and D_2, assume homologous motion throughout the nuclear-burning shell. Numerical models show that actually the hydrogen burning shell is *the* region of the star where homologous change is least satisfied ($0.7 \lesssim -4 * \delta\ln r/\delta\ln P \lesssim 0.9$) [4], nonetheless the deviations from homology are small enough for the instability conditions to remain predictive.

[4] $\delta\ln Q \equiv \ln Q(m,t_1) - \ln Q(m,t_0)$, i.e. a Lagrangian temporal difference of quantity Q.

The variation of the determinants D_1 (black) and D_2 (gray) as determined in diffusive $0.19\,M_\odot$, $Z = 0.02$ models during their thermally pulsing phase are presented in Fig. 9. The behavior of the two quantities is representative for all other cases we studied for this exposition. The actual magnitude of the discriminants, in particular of D_2, depends on the details of how the hydrogen-burning shell is defined. For Fig. 9, the region with $\varepsilon_{\rm nuc} > \varepsilon_{\rm crit} \equiv 5$ erg/g/s is assumed to measure the extension of the hydrogen-burning shell. The physical quantities entering the stability criteria are evaluated at the bottom of the shell as this is the dominant location for the analysis. The thermodynamic quantities in D_1 and D_2 do not vary strongly across the shell, this applies in particular for the quantities entering D_1; even the measure $\Delta r/r$ is robust since the nuclear-burning shell is geometrically thin. On the other hand, all the quantities in the denominator of D_2 in Eq. (2) depend on varying degree on the particular choice of $\varepsilon_{\rm crit}$.

The variation of D_1 during the flash cycle is dominated by the quantity $\Delta r/r$ of the nuclear burning shell, which can also be discerned clearly in the Kippenhahn diagrams of Fig. 6. It is also the

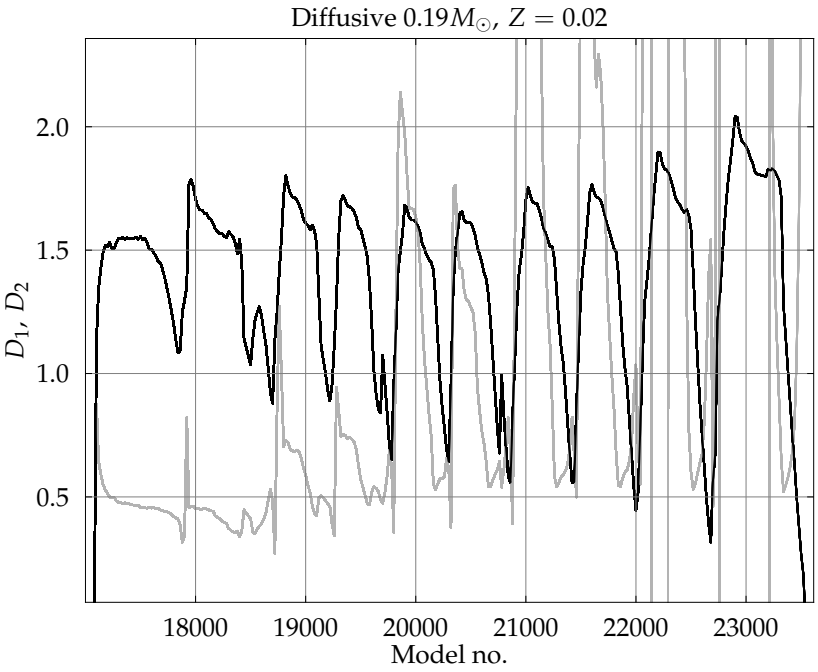

Figure 9: Temporal evolution of the stability discriminants D_1 (black line) and D_2 (gray line) during the H-shell flash phase of the diffusive $0.19 M_\odot$, $Z = 0.02$ model sequence. The size of the nuclear burning shell was determined at $\varepsilon = 5$ erg/g/s level.

monotonously shrinking value of $\Delta r/r$ which lets D_1 eventually to tend to zero. The variability of $1/\Gamma_1 \equiv \alpha - \nabla_{\rm ad} \cdot \delta$ is small and is not important for the functional behavior or the amplitude of the variability of D_1. In particular, Γ_1 of the hydrogen-burning shell does not change systemically during the evolution through the thermal-pulse phase.

The magnitude, but not the amplitude of variability of ε_T is important for instability in condition D_2. The range $12 \lesssim \varepsilon_T \lesssim 17$ as measured in all models of all analyzed sequences points unambiguously at *CNO burning as the dominating nuclear energy source* in the shell. In particular, ε_T stays that high at the end of the thermal pulsing phase also in the least massive studied models which we computed. Put otherwise, the young white dwarfs turn secularly stable before their ever weakening nuclear burning becomes *pp*-burning dominated. It is the cyclic variation of $\Delta L/L$, evaluated at the edges of the nuclear burning shell, which dominates variability of D_2. Additionally, the long-term change of the temperature contrast, $\Delta \ln T$, across the shell contributes to the ever rising trend of D_2 which underlies its cyclic variability.

For the model sequence under consideration in Fig. 9, criterion D_1 in particular is observed to not develop a sufficiently deep minimum at the first thermal pulse to correctly predict instability (as seen in the full evolution computations) but it does well for the other eight pulses which were numerically tracked in the full nonlinear evolution computations. Changing the threshold value of $\varepsilon_{\rm crit}$ can remedy this problem, but at the same time this renders the variations of D_2 wilder. In any case, form and amplitude of the *variation* of D_1 and D_2 during the episode of the thermal pulses remain ro-

bust and therefore the criteria are *helpful to understand* the physical processes at work during the secular instability. The sensitivity of the numerical values of D_1 and D_2 on their implementation renders them unpractical to be used directly during evolutionary computations, e.g. for automatic time-stepping choices in stellar-evolution codes.

All in all, we find that for sufficiently massive VLM stars, usually with $M_* \gtrsim 0.32 M_\odot$, have sufficiently fat hydrogen-burning shells during their post red-giant evolution so that the nuclear burning region never becomes secularly unstable. For the mass range roughly $0.2 - 0.35 M_\odot$, the hydrogen-burning shell can get thin enough to trigger one or more hydrogen flashes through the cyclic shrinking of discriminant D_1. The secular instability dies out once the shell weakens enough, a process sped up by the enhanced outward-eating of the shell during the thermal pulses, so that it finally cannot retain enough of the heat perturbation in the shell to feed the thermal runaway; i.e. it is discriminant D_2 which quenches the instability. The low-mass boundary for secular instability is again defined by discriminant D_2 which measures the stabilization via a too weak luminosity and temperature contrast across the hydrogen-burning shell.

The table on the margin lists the lower ($M_{\rm lb}$) and upper mass ($M_{\rm ub}$) boundaries in between of which hydrogen flashes were encountered in our MESA modeling. The column labeled with "Diffusion" indicates if elemental diffusion neglected (×) or was accounted for (✓). The last column lists the heavy-element abundance of the model sequence. The dependency of the mass range of the secular instability on metallicity appears to be stronger than on including/neglecting elemental diffusion in stellar modeling. This observation, before being adopted as a general rule needs support by a much broader computational survey of the relevant parameter space.

$(M_{\rm lb} - M_{\rm ub})/M_\odot$	Diffusion	Z
0.19 - 0.32	×	0.02
0.25 - 0.35	×	0.001
0.175 - 0.36	✓	0.02

Wrap-up

Secular instability of hydrogen-burning shells can be run into by VLM stars under suitable conditions; this has been known for a long time, starting with the findings of Kippenhahn et al. (1968). In the present exposition, the phenomenon was revisited resorting to detailed but exemplary single-star models computed with the MESA stellar evolution code. The results were used to collect pertinent data to foster our understanding of the secular instability of the hydrogen-burning shell.

Above all, hydrogen-shell flashes are a robust phenomenon, they occur for a broad range of chemical compositions, with and without elemental diffusion; hence the inflicted reactions of the stars should be observable at appropriate epochs of the cosmic evolution. Depending on the particular microphysics, i.e. chemical composition,

mixing processes and the like, the phenomenology of the thermal flashes and the stellar mass range that develops secular unstable hydrogen-burning shells varies. Very roughly, VLM star models with secularly unstable hydrogen shells can be found in the mass range roughly between 0.2 and $0.35 M_{\odot}$.

ASTRONOMY IN THE AGING GALAXY is potentially less boring than advocated in the past (e.g. Adams & Laughlin 1997). With regard to the terrestrial civilization, however, *single-star evolution* with its thermally pulsing VLM objects is not relevant. It takes the pertinent VLM stars about $1 - 10 \times 10^{11}$ years to develop their secularly unstable H-burning shells. By then, the sun will have evolved into a faint, cool white dwarf (e.g. Sackmann et al. 1993) probably with only a fragmentary planetary system left, and in particular without a habitable earth. Hence, human civilization on earth is going to miss the light-show that should develop around the Galaxy's retirement from its stelliferous era.

Indifferent to the human possibilities to witness single VLM-star H-flashes, we find that when using the initial mass function (IMF) of Chabrier (2003) for Z=0.02 mass bounds for secular instability, that about 33% of all stars with $M_* < M_{\rm ub}$ will pass through H-shell flashes when the stars with $M_* = M_{\rm ub}$ start flashing. For the case of $Z = 0.001$, the fraction of H-flashing stars drops to about 19%. These numbers are lower boundaries since the star-formation history was no single epoch event. Down to at least about $0.01 M_{\odot}$ the IMF has a negative slope so that the number of H-flashing candidates is huge in the Galaxy. Therefore, the Milky Way should appear quite variable for some time in the Cosmic future, even when it will be made up exclusively by degenerate left-over stellar bodies.

Hence, once the flashing young-white dwarfs brighten up the Milky Way, at least the more metal-rich members are prone to become born-again red giants. A future civilization, even without a heavy stellar-physics history backpack will have another chance to enjoy red-giant like objects; this without ever having seen the by then extinct kind that comes about in our traditional way: As stars evolving away from the main sequence on their way to try to burn helium.

In a population of VLM stars with some spread in stellar formation and a mixture of masses, a future observer of the Galaxy should encounter a mixture of hydrogen-deficient (typically brighter, because the elemental mixing happens during the flash cycle when the VLM stars brighten considerably) and helium-white dwarfs with shallow but very pure hydrogen layers (upon their crossing the instability regions of white dwarfs, asteroseismology – should it still be pursued then – can be predicted to yield measures of superficial H-layer thicknesses of the order of $10^{-3} - 10^{-5}\, M_*$).

The chances for our civilization to witness thermally pulsing single VLM stars are note completely bleak though: The Galaxy might even currently harbor a few candidates. (Kilic et al. 2007) reported

of numerous low-mass white dwarfs for which no indications of a close companion could be observed; the authors argued that super-metal-rich single stars might suffer from enhanced mass-loss when evolving up the 1st giant branch that some stars of the lower-mass fraction do not reach He-ignition and leave the giant branch prematurely to cool then as low-mass helium white dwarfs in less than a Hubble time. However, it seems that only about 50% of $0.4M_\odot$ white dwarfs (Kilic et al. 2007), a number changing to 75% according to the sample analyzed in (Brown et al. 2011), are thought to emerge from the single-star channel. Towards even lower masses, the fraction of pure, single stars sinks rapidly and extremely-low-mass (ELM) white dwarfs with $M_* < 0.2M_\odot$ are expected to be exclusively produced by interactions in close-binary systems as it is illustrated in the next section. Since only white dwarfs with masses approximately $0.2 - 0.35M_\odot$ develop secularly unstable H-burning shells, and those close to the low-mass boundary are the most "violent" and hence the most flamboyant ones, only a tiny fraction, if at all, of low-mass helium white dwarfs remain as candidates at the end of the exclusion process.

There is observational evidence from the populations of red giants in stellar aggregates such as globular clusters and the local neighborhood in the Galaxy that red-clump giants are underabundant or even missing as [Fe/H] increases. See Kilic et al. (2007) for references.

In close binary stars in which mass is abstracted from the primary component via evolution scenario A or B, the donor can turn into a low-mass star unable to ignite core helium burning. Within a fraction of a Hubble time, such stars can end up as low-mass or even ELM helium white dwarfs. The initial *modeling* with evidence for H-shell flashes was found just in this framework (Kippenhahn et al. 1968).

Hints at the binary channel to produce low-mass helium white dwarfs come already from the entrance, i.e. from VLM *subdwarfs* and *proto white-dwarfs* in close binary systems, which were discovered and monitored in the recent past. Maxted et al. (2012) reported on the mass determinations of the components of the double-lined eclipsing system J0247-25 and their Fig. 5 presents the distribution of nine yet calibrated low-mass binary components on the HR plane and their relation to stellar evolution tracks adopted from the earlier modeling literature. The photometric space mission *Kepler* yielded recently a very intriguing low-mass star that must have shortcut the ascent of the 1st giant branch and which is presently observed to cross the classical instability strip and is observable as an RR Lyrae – type pulsating variable[5] (Pietrzyński et al. 2012). The low-mass pulsator should evolve into a hot white dwarf within about the next 10^7 years and, based on the estimated mass, pass through at least one hydrogen-shell flash.

The large-scale sky survey SDSS reveals the ubiquity of ELM white dwarfs (e.g. Brown et al. 2012; Kilic et al. 2012) in the Galaxy. Even the first three examples of old ELM white dwarfs[6] which have cooled down into the ZZ Ceti instability strip were recently reported by Hermes et al. (2012, 2013). Depending on the richness of the eventually recoverable frequency spectra of the pulsators an astero-

[5] The system RRLYR-02792 is a detached, double-line eclipsing binary with the primary component, the pulsating star, being observed with a mass of $0.26M_\odot$. The secondary component is attributed a mass of $1.67M_\odot$. The two stars orbit each other every 15.24 days; the pulsation period of the primary star is 0.627 days. About ten years of monitoring shows the period to clearly decrease ($\dot{P} = -8.4 \times 10^{-6}$ days/year) indicating a blueward evolution of the star – just as expected by the invoked scenario.

[6] SDSS J184037.78+642312.3
SDSS J151826.68+065813.2
SDSS J111215.82+111745.0

seismic probing of the thickness of their hydrogen-rich surface layer can be anticipated.

Observational evidence of ELM white dwarfs in double degenerates – either in double white-dwarf systems (DWD) or in white-dwarf / neutron-star pairs, in particular if the neutron star is a millisecond pulsar (MSP), has amassed over the past few years (e.g. Kilic et al. 2012; Marsh 2011, and references therein to earlier achievements).

DWD SYSTEMS are at the center of considerable research activity since, if they are sufficiently tightly bound and can merge within a fraction of the age of the Cosmos, time and again they are traded as candidates for type Ia supernovae (if the components are CO white dwarfs, i.e. the components are massive enough) and sources of gravitational waves, which might soon become detectable by the detectors of the LIGO/VIRGO experiments.

The binary nature of low-mass white dwarfs has been observationally established in the outgoing 20th century, starting with Marsh et al. (1995) (finding white-dwarf masses of $\sim 0.3 - 0.4\,M_\odot$) and was thereafter supported and extended (also towards lower white dwarf masses ; i.e. $\lesssim 0.2\,M_\odot$, see references in Kaplan et al. (2012) by larger samples collected in surveys such as the SDSS (e.g. Kilic et al. 2011). DWD systems having endured multiple common-envelope phases might explain the very short-period systems of the extreme kind such as HM Cnc[7] with mass transfer during the inspiraling of the two white dwarf components. Eventually, such binary systems might evolve into helium mass-transferring cataclysmic AM CVn stars (Kaplan et al. 2012).

[7] also known as RX J0806.3+1527, an X-ray source discovered with ROSAT in 1999. The binary system consists of two white dwarfs, each of about $0.5\,M_\odot$ with an orbital period of 5.4 minutes!

ELM white dwarfs are predicted to possess stably burning H envelopes ($M_{\rm env} \sim 10^{-3} - 10^{-2} M_\odot$) which let them stay bright for $\mathcal{O}$(Gyr) (Serenelli et al. 2002; Panei et al. 2007); this can be understood from the fact that no hydrogen flashes can occur which quickly reduce the H-rich envelope mass. Apparently, for the DWD system NLTT 11748, the geometric measurement of the radius of an ELM candidate was possible Kawka & Vennes (2009), yielding $0.04\,R_\odot$ for an $0.15\,M_\odot$ He white dwarf; a value which appears to be compatible with a thick stably burning hydrogen envelope.

With respect to cooling ages and possibly other observables, we expect a split-up of the population of low-mass white dwarfs: The mass range of thermally pulsing low-mass helium white dwarfs is expected to have thin H-rich/H-pure envelopes and short cooling ages; on the other hand the thermally stable VLM/ELM He white dwarfs that burn hydrogen stably can live with thick H-rich envelopes and sustain significant luminosity over long times and hence appear older at a given luminosity.

MSP SYSTEMS constitute one group of double degenerate binary systems that contain a VLM white dwarf with $M_* \lesssim 0.4\,M_\odot$ and a

neutron star with mass of the order of $1.5\,M_{\odot}$. Due to its very low mass, the white dwarf is thought to have a helium core with a thin hydrogen blanket. The neutron star is thought to have been spun up through angular-momentum transfer during earlier mass-exchange episodes. Therefore, in this framework the MSP birth epoch is taken to coincide with the start of the "cooling" of the low-mass white dwarf that emerged from the mass-loss episode. Hence, the cooling time (the time from starting on the cooling sequence of He white dwarfs) and the spin-down age of the MSP must coincide. A problem that hampered MSP understanding in the past was the incompatibility of the model-derived age of the white dwarf component and of that of the MSP.

As discussed in Althaus et al. (2001, and references therein), and reiterated by Benvenuto & De Vito (2005), who also computed the orbital evolution of the binary system, the inclusion of elemental diffusion in modeling the white dwarf evolution proved essential to reduce the cooling age of the white-dwarf companion of MSPs and to reconcile their ages. If white dwarfs harbor thick envelopes, such as they develop in diffusion-free models, the degenerate stars cool too slowly since hydrogen burning can maintain the star's luminosity for a too long period of time. On the other hand, accounting for elemental diffusion allows already the pre-white dwarfs to burn their hydrogen more efficiently due to the purified burning shells. Since hydrogen flashes are encountered also in white-dwarf models in which elemental diffusion was accounted for, this process opens additional ways to effectively reduce the amount of superficial H-rich material: Hydrogen flashes rapidly burn H to He and reduce the thickness of the H-rich envelope from the bottom. Furthermore, if the flash forces the star to puff up and to expand possibly beyond its Roche radius the then starting rapid mass-loss can reduce the thickness of the H-rich envelope by stripping it from the top. Any of these processes forces a H-flashing star to further speed up its cooling because it has less fuel to support its nuclear furnace (e.g. Althaus et al. 2001). Ergma et al. (2001) contemplated the possibility of irradiation by the neutron star to play a potentially significant rôle to chip away hydrogen-rich superficial matter from the white dwarf when it is inflated during a hydrogen flash.

Since not all VLM/ELM helium white dwarfs undergo H-flashes, they only contribute partially to the solution of the clocking problem in MSPs which was discussed above. Hence it should be very interesting to strive for large enough samples of MSPs with calibrated white-dwarf companion masses. In particular around the boundaries that separate the H-flashing domain from the high- and low-mass stably burning VLM/ELM white dwarfs, an enhanced age spread should be observable. The data might be useful to scrutinize the involved microphysics that determines structure and stability of the H-burning shell. If VLM/ELM white dwarfs in MSP systems even happen to fall into one of the white dwarfs' instability strips, asteroseismology will be a ready tool to probe the envelope struc-

tures and might supply an independent measure of the hydrogen-layer thickness.

AN OUTLOOK ON MORE MASSIVE STARS, still of the low-mass kind but having entered helium burning at some stage during their evolution, reveals that they too can run into unstable hydrogen-burning shells under suitable circumstances during the post-AGB stage. One mechanism was promoted by Iben & MacDonald (1986): Young white dwarfs that left the AGB during either He-shell or early H-shell burning manage to contaminate their essentially pure helium mantle with ^{1}H and ^{12}C through chemical diffusion. If the accumulation of C, N, and H become favorable in the right temperature window, unstable CNO-burning can emerge. The lightcurve produced by the resulting thermal flash appeared to be reminiscent of very slow novae so that the authors referred to the phenomenon as a *self-induced nova*. Miller Bertolami et al. (2011) who computed more self-contained white-dwarf models with proper antecedents revisited the scenario, rebaptizing it to the more designative *diffusion-induced nova*, to scrutinize it with a wider range of constitutional parameters. The stability behavior of the CNO-burning shell was paid attention to by applying the formalism which was used earlier on by Yoon et al. (2004) who relied on the local linear-stability ansatz of Giannone & Weigert (1967). The secular shell instability that leads to diffusion-induced novae can be understood along the same line of arguments as presented in this exposition.

ACKNOWLEDGMENTS This exposition relied heavily on NASA's Astrophysics Data System Bibliographic Services. The value of the efforts of Bill Paxton and the MESA community to make available to the student of the stars, irrespective of affiliation and status, an open-source one-of-a-kind stellar evolution code such as MESA can hardly be overstated. Hideyuki Saio and Leandro Althaus generously donated of their time to read through the exposition with critical eyes.

Appendix: Star Modeling

The stellar models referred to and analyzed in this exposition were all computed with the MESA code in its version 4298 (cf. Paxton et al. 2011, 2013, for a general description of the MESA project). Convection was treated with the Henyey scheme assuming an ad hoc mixing-length of 1.8 pressure scale-heights. The choice $Z = 0.02, X = 0.7$, as an example of PopI abundances, allowed the sequence of homogeneous models to start from initial models located close to the ZAMS. For the exemplary PopII abundances, chosen as $Z = 0.001, X = 0.757$, the evolution computations were

For the opacity data, `gn93` and `lowT_fa05_gs98` tables at low temperatures were requested in MESA. The EoS was computed with `macdonald` data for its smoothness.

started with homogeneous pre-main-sequence polytropes, which first contracted along the Hayashi track onto the ZAMS to be then followed up to their terminal cooling stage as helium white dwarfs.

Elemental diffusion in MESA is treated for the species under consideration by solving Burgers' equation in parallel to the stellar structure/evolution equations, the implementation in MESA is comparable to that described in Althaus & Benvenuto (2000).

`do_element_diffusion = .true.` was set in the `&controls` section of the inlist; we adopted the default settings from `star_defaults.dek` with 5 species classes that were used for the diffusion computations.

References

Adams, F. C. & Laughlin, G. 1997, Rev. Mod. Phys., 69, 337

Althaus, L. G. & Benvenuto, O. G. 2000, MNRAS, 317, 952

Althaus, L. G., Serenelli, A. M., & Benvenuto, O. G. 2001, MNRAS, 323, 471

Benvenuto, O. G. & De Vito, M. A. 2005, MNRAS, 362, 891

Brown, J. M., Kilic, M., Brown, W. R., & Kenyon, S. J. 2011, ApJ, 730, 67

Brown, W. R., Kilic, M., Allende Prieto, C., & Kenyon, S. J. 2012, ApJ, 744, 142

Chabrier, G. 2003, PASP, 115, 763

Driebe, T., Blöcker, T., Schönberner, D., & Herwig, F. 1999, A&A, 350, 89

Driebe, T., Schönberner, D., Blöcker, T., & Herwig, F. 1998, A&A, 339, 123

Ergma, E., Sarna, M. J., & Gerškevitš-Antipova, J. 2001, MNRAS, 321, 71

Giannone, P. & Weigert, A. 1967, ZfA, 67, 41

Hermes, J. J., Montgomery, M. H., Winget, D. E., et al. 2013, ApJ, 765, 102

—. 2012, ApJL, 750, L28

Iben, I. 2013, Stellar Evolution Physics: Advanced Evolution of Single Stars (Cambridge University Press)

Iben, I. & MacDonald, J. 1986, ApJ, 301, 164

Kaplan, D. L., Bildsten, L., & Steinfadt, J. D. R. 2012, ApJ, 758, 64

Kawka, A. & Vennes, S. 2009, A&A, 506, L25

Kilic, M., Brown, W. R., Allende Prieto, C., et al. 2011, ApJ, 727, 3

—. 2012, ApJ, 751, 141

Kilic, M., Stanek, K. Z., & Pinsonneault, M. H. 2007, ApJ, 671, 761

Kippenhahn, R., Kohl, K., & Weigert, A. 1967, ZfA, 66, 58

Kippenhahn, R., Thomas, H.-C., & Weigert, A. 1968, ZfA, 69, 265

Kippenhahn, R. & Weigert, A. 1994, Stellar Structure and Evolution (Springer)

Marsh, T. R. 2011, Class. Quantum Grav., 28, 4019

Marsh, T. R., Dhillon, V. S., & Duck, S. R. 1995, MNRAS, 275, 828

Maxted, P. F. L., Anderson, D. R., Burleigh, M. R., et al. 2012, in ASP Conference Series, Vol. 452, Fifth Meeting on Hot Subdwarf Stars and Related Objects, ed. D. Kilkenny, C. Jefferey, & C. Koen (Astronomical Society of the Pacific), 137

Miller Bertolami, M. M., Althaus, L. G., Olano, C., & Jiménez, N. 2011, MNRAS, 415, 1396

Paczyński, B. 1975, ApJ, 202, 558

Panei, J. A., Althaus, L. G., Chen, X., & Han, Z. 2007, MNRAS, 382, 779

Paxton, B., Bildsten, L., Dotter, A., et al. 2011, ApJS, 192, 3

Paxton, B., Cantiello, M., Arras, P., et al. 2013, arXiv:1301.0319v1

Pietrzyński, G., Thompson, I. B., Gieren, W., et al. 2012, Nature, 484, 75

Sackmann, I.-J., Boothroyd, A. I., & Kraemer, K. E. 1993, ApJ, 418, 457

Sarna, M. J., Ergma, E., & Gerškevitš-Antipova, J. 2000, MNRAS, 316, 84

Schwarzschild, M. & Härm, R. 1965, ApJ, 142, 855

Serenelli, A. M., Althaus, L. G., Rohrmann, R. D., & Benvenuto, O. G. 2002, MNRAS, 337, 1091

Yoon, S.-C., Langer, N., & van der Sluys, M. 2004, A&A, 425, 207